Journal of Materials Chemistry B

Accepted Manuscript

This is an *Accepted Manuscript*, which has been through the Royal Society of Chemistry peer review process and has been accepted for publication.

Accepted Manuscripts are published online shortly after acceptance, before technical editing, formatting and proof reading. Using this free service, authors can make their results available to the community, in citable form, before we publish the edited article. We will replace this *Accepted Manuscript* with the edited and formatted *Advance Article* as soon as it is available.

You can find more information about *Accepted Manuscripts* in the Information for Authors.

Please note that technical editing may introduce minor changes to the text and/or graphics, which may alter content. The journal's standard Terms & Conditions and the Ethical guidelines still apply. In no event shall the Royal Society of Chemistry be held responsible for any errors or omissions in this *Accepted Manuscript* or any consequences arising from the use of any information it contains.

ROYAL SOCIETY OF CHEMISTRY

www.rsc.org/materialsB

Cite this: DOI: 10.1039/c0xx00000x

www.rsc.org/xxxxxx

ARTICLE TYPE

Combination delivery of Adjudin and Doxorubicin via integrating drug conjugation and nanocarrier approaches for the treatment of drug-resistant cancer cells

Xu Li [a], Cuixia Gao [a], Yupei Wu [a], C-Yan Cheng [b], Weiliang Xia [c] and Zhiping Zhang [a,*]

Received (in XXX, XXX) Xth XXXXXXXXX 20XX, Accepted Xth XXXXXXXXX 20XX
DOI: 10.1039/b000000x

Combination therapy has been regarded as a potent strategy to overcome multidrug resistance (MDR). In this study, we adopt Adjudin (ADD), a mitochondria inhibitor, and Doxorubicin (DOX), a common chemo-drug, to treat drug-resistant cancer cells (MCF-7/ADR) in combination. Given the different physico-chemical properties of ADD and DOX, we develop a novel drug formulation (ADD-DOX (M)) by integrating drug conjugation and nanocarrier approaches to realize the co-delivery of such two drugs. We demonstrate the conjugation of ADD and DOX via forming acid-sensitive hydrazone bond, and then the encapsulation of ADD-DOX conjugates by DSPE-PEG_{2000} micelles with high drug encapsulation efficiency and well-controllable drug loading efficiency. The obtained ADD-DOX (M) micelles are found to be stable under physiological condition, but can rapidly release drugs within acidic environments. Following cellular experiments confirm that, ADD-DOX (M) vehicles can be internalized by MCF-7/ADR cancer cells through endocytic pathway and exist within the moderate acidic endolysosomes, thus accelerating the hydrolysis of ADD-DOX and the release of free ADD and DOX. As a result, the ADD-DOX (M) formulation exhibits excellent anti-MDR effect. In summary, we for the first time report the combinational use of ADD and DOX with an effective co-delivery strategy for the treatment of MDR cancer cells.

Introduction

Multidrug resistance (MDR) is among the major reasons for the failure of clinic chemotherapy and still remains a huge challenge in cancer treatment. [1] Applying specific regulators, such as P-glycolprotein inhibitors (P-gp) or MDR-associated gene suppressors, to enhance the chemo-sensitivity of drug-resistant cancer cells has been proven to be a promising strategy to overcome MDR. [2-5] Therefore, combinational use of MDR regulators and chemo-drugs triggers great research interests for enhanced MDR cancer therapy. [6-8] Recent studies have suggested that mitochondria are potent targets to reverse MDR phenotype. [9, 10] Agents that cause mitochondrial damage can impede the energy metabolism and/or down-regulate the expression of anti-apoptotic proteins, thereby restoring the chemosensitization of MDR cancer cells. These thus set a solid basis for using mitochondria-targeting agents and common chemo-drugs in combination to treat MDR cancers.

Adjudin (ADD) is an extensively studied male contraceptive with superior mitochondria-inhibitory effect. [11, 12] Since its analogue Lonidamine (LND) is a well known anticancer drug, the anticancer capability of ADD has been recently evaluated by Xie and colleagues. [13] It was found that, in a variety of cancer cell lines, ADD could mediate cellular apoptosis via causing mitochondrial dysfunction. Moreover, the anticancer activity of ADD was 3-9 folds higher than that of LND. Accordingly, ADD possesses great potential to serve as a mitochondria-targeting anticancer agent. Doxorubicin (DOX), an inhibitor of DNA replication, is one of the leading antitumor chemo-drugs with excellent capability against a wide broad of cancers. [14] However, clinic studies have demonstrated that MDR seriously reduced the therapeutic efficacy of DOX. [15, 16] Therefore, in this work, we seek to use ADD to enhance DOX-related MDR cancer chemotherapy. Given the different physico-chemical properties (such as solubility) of ADD (poorly soluble) and DOX (well soluble), key for this combination therapy should be an effective co-delivery strategy that ensures simultaneous accumulation of abundant individual drug molecules in cancer cells.

Nanocarriers provide an innovative platform for the delivery of small-molecule chemo-drugs. [17, 18] In particular, nanocarriers consisting of conventional excipients that certified for human use (such as lecithin, poly lactic-co-glycolic acid (PLGA), etc.) have aroused broad research interest, due to their good biocompatibility, high safety and great potential for clinic application. [19, 20] Nevertheless, it presents a challenge for conventional nanocarriers to co-encapsulate both hydrophobic and hydrophilic agents. [21, 22] For instance, biodegradable solid nanoparticles, such as those prepared by PLGA, possess good stability and well controllable drug release characteristics, but they are not suitable for loading well-soluble drugs, not to

Journal of Materials Chemistry B Accepted Manuscript

mention relative combination delivery; on the other hand, liposomes can package hydrophilic and hydrophobic drugs in its inner core and bilayer membrane, respectively, but this formulation has disadvantages such as low stability, limited drug loading efficiency (especially for the hydrophobic drugs) and uncontrollable drug leakage. [23-25] Consequently, direct co-delivery of ADD and DOX by conventional nanocarriers is difficult to achieve.

Drug conjugation approach offers a resolution to diminish the influence of the varying physico-chemical properties of individual drugs. [26-28] Since drug conjugate is a single entity, it can be readily encapsulated and delivered by conventional nanocarriers. [21, 29] Therefore, we herein integrated the drug conjugation and nanocarrier approaches to realize the co-delivery of ADD and DOX. We reported the synthesis and characterization of the conjugate of ADD and DOX, termed as ADD-DOX, which possessed acid-responsive hydrolysis characteristic. We then demonstrated that ADD-DOX could be readily packaged by a type of conventional nanocarriers, DSPE-PEG_{2000} micelles, with high drug encapsulation efficiency and well-controllable drug loading efficiency. We also confirmed that the obtained delivery vehicles, denoted as ADD-DOX (M), were stable under physiological pH value, but could rapidly release free individual drugs within moderate acidic environment. In following cellular experiments, we verified that ADD-DOX (M) was internalized into cells through endocytic pathway and exhibited excellent anti-MDR capability. Note that the emphasis of this work is to present the effective co-delivery of ADD and DOX for combinational MDR treatment, rather than to demonstrate the optimized synergistic effects between such two drugs.

Experimental Section

Reagent

Adjudin (ADD) was synthesized at S.B.M. Srl (Rome, Italy) with a purity of >98% as described earlier. [30] Doxorubicin hydrochloride (DOX·HCl) was purchased from Huafeng United Technology CO., Ltd (Beijing, China). 1, 2-distearoyl-*sn*-glycero-3-phosphoethanolamine-N-[methoxy (polyethylene glycol)-2000] (DSPE-PEG_{2000}) was obtained from Avanti Polar Lipids Inc. (Alabaster, AL, USA). DMSO for cellular experiments was purchased from Sigma–Aldrich (St. Louis, MO, USA). Lysotracker Green DND-26 was purchased from Invitrogen (Carlsbad, CA, USA). 3-(4, 5-dimethylthiazol-2-yl)-2, 5-diphenyl tetrazolium bromide (MTT) and Hoechst 33258 were purchased from Biosharp (Seol, South-Korea). The ATP Bioluminescence Assay Kit and the BCA Protein Assay Kit were from Beyotime Institute of Biotechnology (Shanghai, China). RPMI-1640 medium, Penicillin−streptomycin, fetal bovine serum (FBS) and trypsin without EDTA were purchased from Hyclone (USA). All other non-mentioned reagents were obtained from Aladdin (Shanghai, China).

Synthesis of ADD-DOX conjugates

ADD (10.0 mg) and DOX·HCl (5.8 mg) with molar ratio 3:1 were co-dissolved in 2 mL methanol with 0.5% (v/v) trifluoroacetic acid (TFA), and kept reaction with stirring in darkness at room temperature. After 12 h, the solution was evaporated under reduced pressure at room temperature to remove the organic solvent. The residue was re-dissolved with 0.3 mL methanol, and then 4.5 mL ethyl acetate was added dropwise into the methanol solution to allow precipitation. The precipitate was collected by centrifugation at 2000 g and further purified by recrystallization methods as early described. [31, 32] The final obtain red solid was dried at 30 ºC under vacuum and stored in a desiccators before use (yield of 6.5 mg, ~65.5%). ^{1}H-NMR (400 MHz, DMSO-d_6), δ (ppm), 13.9, (br, 1H), 13.2, (br, 1H), 12.2 (s, 1H), 8.4-6.8 (m, 12H), 6.3 (s, 1H), 5.7 (s, 2H), 5.5 (d, 1H), 5.3 (s, 1H), 5.2 (s, 1H), 5.1 (s, 1H), 4.6 (m, 2H), 4.1 (m,1H), 3.9 (s, 3H), 3.6 (s, 1H), 3.4 (d,1H), 3.2-2.8 (dd, 2H), 2.2 (m, 2H), 1.8-1.6 (m, 2H), 1.3 (d, 3H); ^{13}C-NMR (DMSO-d_6), δ (ppm), 17.3, 28.75, 33.52; 38.66, 47.08, 50.1, 56.95, 58.68, 66.53, 66.69, 71.72, 72.28, 99.81, 110.78, 110.85, 111.08, 119.24, 119.9, 120.12, 122.14, 122.87, 123.58, 127.82, 128.21, 129.49, 131.35, 133.48, 133.66, 133.85, 134.87, 135.57, 136.17, 136.5, 137.31, 141.35, 155.14, 156.76, 158, 158.9, 161.07, 186.48, 186.6; HR-ESI-MS: m/z Calcd $[M+H]^+$ 860.2101, Found 860.2095; Anal Calcd for $[C_{42}H_{39}Cl_2N_5O_{11}\cdot CF_3COOH]$: C, 54.2; N, 7.18; H, 4.16; found: C, 54.16; N, 7.29; H, 4.45.

Characterization of ADD-DOX conjugates

The purity was evaluated by high performance liquid chromatography (HPLC) through using a Hitachi UV detector L-2400 system (Japanese) with a reversed-phase column (Viva-C18, particle size 5 μm; 150 mm × 4.6 mm, Restek, USA). Elution was monitored by UV absorbance at 298 nm under isocratic conditions (mobile phase: water/methanol/acetic acid, 11/88/1, v/v/v). The mass and molecular formula were evaluated by high-resolution electrospray ionization mass spectrometry (HR-ESI-MS, Bruker micrOTOF, Switzerland) with a positive mode. The structure information was analyzed by ^{1}H and ^{13}C nuclear magnetic resonance (NMR) via using a Bruker AM-400 spectrometer (Switzerland). The spectra of Fourier transform infrared (FTIR) and ultraviolet-visible (UV) spectroscopies were analyzed by a Bruker VERTEX-70 spectrophotometer (Germany) and a Shimadzu UV probe spectrometer (Japanese), respectively. The emission and excision fluorescence property were determined by Hitachi F-4600 FL Spectrophotometer (Japanese). The elemental analysis was carried out by using a Vario EL cube instrument (Elementar, Germany).

Hydrolysis profile of ADD-DOX

A hydrolysis study of ADD-DOX was performed to confirm that it could be hydrolyzed into individual drugs, and to determine the corresponding hydrolysis kinetics under different pH values. ADD-DOX conjugates were dissolved in a mixed solution of water/methanol (75/25, v/v) with different pH values of 4.0, 5.2, 6.5 and 7.4, respectively. After incubation at 37 ºC for preconcerted time period (ranging from 0.5 to 48 h), an aliquot of the sample in each group was separated and subjected to HPLC with mobile phase of water/methanol/acetic acid (21/78/1, v/v/v) to determine the hydrolysis ratio.

Preparation and characterization of ADD-DOX (M)

ADD-DOX (M) was prepared through a film dispersion method as described. [33, 34] In brief, 2 mg ADD-DOX conjugates and 10 mg DSPE-PEG_{2000} were co-dissolved in 2 mL methanol. After

This journal is © The Royal Society of Chemistry [year]

Journal of Materials Chemistry B Accepted Manuscript

incubation for 30 min, the organic solvent was removed by evaporation under reduced pressure at room temperature. Then, the as-prepared uniform film was hydrated with 1 mL double-distilled water or phosphate-buffered saline (PBS, pH 7.4), followed by vigorous vortex for 1 min and incubation at 60 ºC for 30 min. The obtained micelles suspension was filtrated through a 200 nm polycarbonate membrane (Millipore Co., Bedford, MA, USA) and stored in 4 ºC before characterization and cellular experiments.

To evaluate the encapsulation efficiency and the drug-loading efficiency, lyophilized samples of ADD-DOX (M) were re-dissolved with methanol, and then the quantity of ADD-DOX was determined by fluorescence spectrometer. We prepared a type of ADD-DOX (M) with DLE of 16.7% for the following characterization and cellular experiments. The morphology of ADD-DOX (M) was observed by Transmission Electron Microscopy (TEM, Tecnai G2 20 U-TWIN, FEI Co., USA). The hydrodynamic size and zeta potential of such micelles was determined by dynamic light scattering (DLS) method (Zeta Plus, Brookhaven, USA).

Drug release profile of ADD-DOX (M)

The drug release behaviors of ADD-DOX (M) were determined by dialysis method via using a membrane with molecular weight cut-off of 3,500 Da. 0.5 mL ADD-DOX (M) (equivalent with ADD-DOX concentration of 0.25 mM) was dialysis against 50 mL outer phase (20 mM PBS with pH value of 5.0 or 7.4). After incubation at 37 ºC for pre-designed time period (arranging from 1 to 72 h), 5 mL sample was withdrawn in each group and replaced with 5 mL fresh outer phase. The concentrations of DOX in outer phase were determined by fluorescent spectrophotometry. To determine the concentrations of ADD, drugs were extracted from separated outer phase by dichloromethane, followed by measurement with HPLC. Each drug release profile was expressed as the percentage of the total quantity of individual drug and plotted as a function of time.

Cell culture

MCF-7 and MCF-7/ADR cell lines, served as drug-sensitive and drug-resistant cancer cells, respectively, were donated by Prof. Yaping Li (Shanghai Institute of Materia Medica, Chinese Academy of Sciences) and cultured in RPMI-1640 medium supplemented with 10% (v/v) FBS and 1% (v/v) penicillin-streptomycin solution. For MCF-7/ADR cells, the medium also contained 1 μg/mL DOX to maintain the acquired drug resistance. The above cell cultures were incubated in a CO_2 incubator at 37 ºC in a humidified atmosphere with 95% air/5% CO_2.

Cellular uptake experiments

To assess cellular uptake of drugs, confocal laser scanning microscopy (CLSM, Zeiss Axio Observer, Carl Zeiss, Germany) was used. In brief, MCF-7/ADR cells or MCF-7 cells were seeded in cover slip-loaded 24-well plates at a density of 1×10^5 cells per well. After incubation for 24 h, culture medium was replaced by fresh medium containing ADD-DOX (M) or DOX (with drug concentration of 5 μM and 40 μM, respectively). Thereafter, cells were incubated for specified time periods of 1, 4, 12, 24 or 48 h, and then treated with 4% paraformaldehyde and Hoechst 33258 for fixation and nuclei staining, respectively. Treated cells on cover slips were then mounted on glass slides in glycerol.

For determination of the mean fluorescence intensity in cells by flow cytometry (FCM, FACScadibur, BD, USA), MCF-7/ADR cells were seeded in 12-well plates at a density of 2×10^5 cells/well. After 24h of incubation, cells were exposed to medium containing ADD-DOX (M) (equivalent with ADD-DOX concentration of 5 μM). Untreated cells severed as the negative control. At specific incubation time points of 1, 4, 8, 12 and 24 h, cells were trypsinized and collected by low speed centrifugation. Finally, the separated cells were resuspended in ice-cold PBS and analyzed by FCM subsequently. Two independent measurements were performed and each sample had duplicates.

The energy-dependent endocytosis of ADD-DOX (M) was investigated through comparing the intracellular fluorescence for cellular internalization occurring at different temperatures. MCF-7/ADR cells were pre-incubated at 4 ºC or 37 ºC for 1 h, and then treated with medium containing ADD-DOX (M) (with 40 μM ADD-DOX) at the same temperature for another 1 h. Thereafter, cells were characterized by qualitative CLSM imaging and quantitative flow cytometry analysis.

Subcellular localization study

MCF-7/ADR cells were seeded in 24-well plates with cover slips at density of 1×10^5 per well. After 24 h of incubation, cells were exposed to ADD-DOX (M) (equivalent with 40 μM ADD-DOX) for 4 h. Thereafter, cells were treated with 200 nM Lysotracker Green DND-26 for 20 min, followed by exposure to 4% paraformaldehyde for 10 min. These cells were then incubated with Hoechst 33258 for nuclei staining. Finally, the treated cells on cover slips were mounted on glass slides in glycerol and observed by CLSM.

Cellular viability assay

A standard MTT assay was used to assess the cytotoxicity of ADD-DOX (M). In detail, MCF-7/ADR or MCF-7 cells were seeded in 96-well plates with a density of 5×10^3 cells/well, followed by incubation for 24 h. Thereafter, cells were treated with medium containing serial concentrations of drugs. After 72 h of incubation, cells were washed with PBS twice and exposed to 100 μL MTT-contained serum-free medium (0.5 mg/mL) for 2 h at 37 ºC. Then, the culture medium was discarded and replaced by 150 μL DMSO for dissolving the generated formazan. After 15 min of incubation, the absorbance at 570 nm was determined in each well by using a multi-mode microplate reader (Synergy™ HT, Bio Tek, USA). The half-maximal inhibitory concentrations (IC_{50}) were calculated by SPSS software and the corresponding resistance factor (denoted as RF) values were determined by the ratio of IC_{50} for drug-resistant cell line to that for its parent drug-sensitive cell line.

Cellular ATP level detection

MCF-7/ADR cells were seeded in 96-well plates with a density of 5×10^3 cells/well, to be followed by 24 h of incubation. Thereafter, cells were exposed to medium containing ADD, DOX, the mixture of ADD and DOX (molar ratio of 1:1) or ADD-DOX (M) micelles for 48 h (with drug concentration at 20 or 60 μM). Thereafter, these cells were treated with lysis buffer to extract ATP and total proteins. The quantity of ATP and proteins in each

Journal of Materials Chemistry B Accepted Manuscript

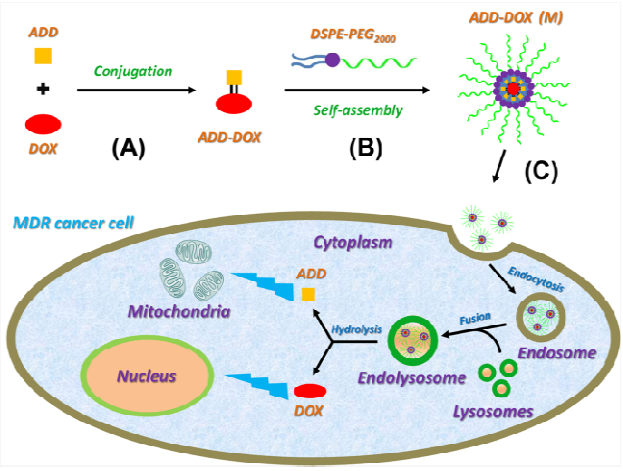

Fig.1. Schematic illustration for the incorporation of drug conjugation approach and nanocarrier technology to co-deliver ADD and DOX for MDR cancer treatments: (A) conjugation of ADD and DOX to synthesize ADD-DOX; (B) mixing ADD-DOX and DSPE-PEG$_{2000}$ to prepare drug-loaded micelles ADD-DOX (M); (C) applying ADD-DOX (M) to treat MDR cancer cells.

sample were determined by ATP luminescence assay and BCA assay, respectively, by using the multi-mode microplate reader (Synergy^{TM} HT, Bio Tek, USA). The measured ATP quantities were normalized against that of the total proteins in the same sample. The final cellular ATP level in each group was expressed as the percentage of that in the control group. Here, 0.2% (v/v) DMSO was added into the medium containing free drugs. For the group of ADD-DOX (M), the measurement was carried out without DMSO. For this experiment, three independent measurements were performed.

Statistical Analysis

The statistical significance of treatment was assessed using the Prism software (GraphPad). The statistical differences were determined by ANOVA, followed by Student's t test. The p values < 0.05 indicate significant differences.

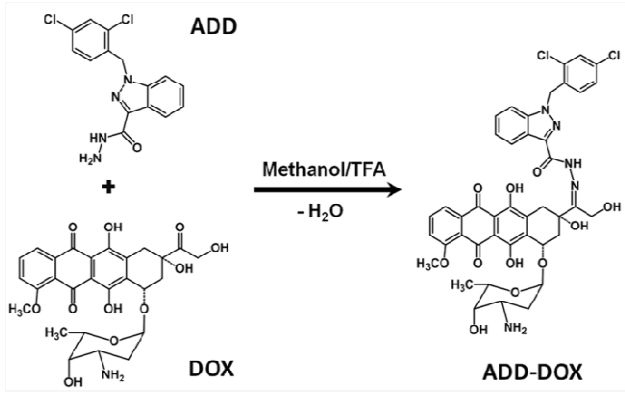

Scheme 1. Synthesis of ADD-DOX via directly conjugating ADD to DOX.

Results and Discussion

Synthesis and characterization of ADD-DOX

Fig.1 described the whole procedure of utilizing ADD and DOX in combination for MDR cancer treatment. We first prepared the drug conjugate of ADD and DOX (Fig. 1, step A). Since ADD contains a hydrazide group and DOX possesses a carbonyl group, such two drugs can directly couple with each other via forming a hydrazone bond. As shown in Scheme 1, the reaction of ADD and DOX was performed in anhydrous methanol with trifluoroacetic acid as catalyst. The obtained crude product was purified by recrystallization method before characterization (purity >95%, HPLC trace seen in Fig. S1).

The formation of ADD-DOX was first confirmed by ^{1}H-NMR spectroscopy with determination of the characteristic peaks and relative integration values of ADD (Fig. S2) and DOX (Fig. S3), respectively. As shown in Fig. 2, peaks at δ=1.3, 3.9 and 4.6 with integration values of 3H, 3H and 2H represented the protons of the methyl groups (C-14, C-4) and the methylene group (C-8) in DOX moiety, respectively. Peaks at δ=5.8, 6.9 and 8.2 with integration values of 2H, 1H and 1H were attributed to the protons of the methylene group (C-19) and the benzene rings (C-20 and C-18) in ADD moiety, respectively.

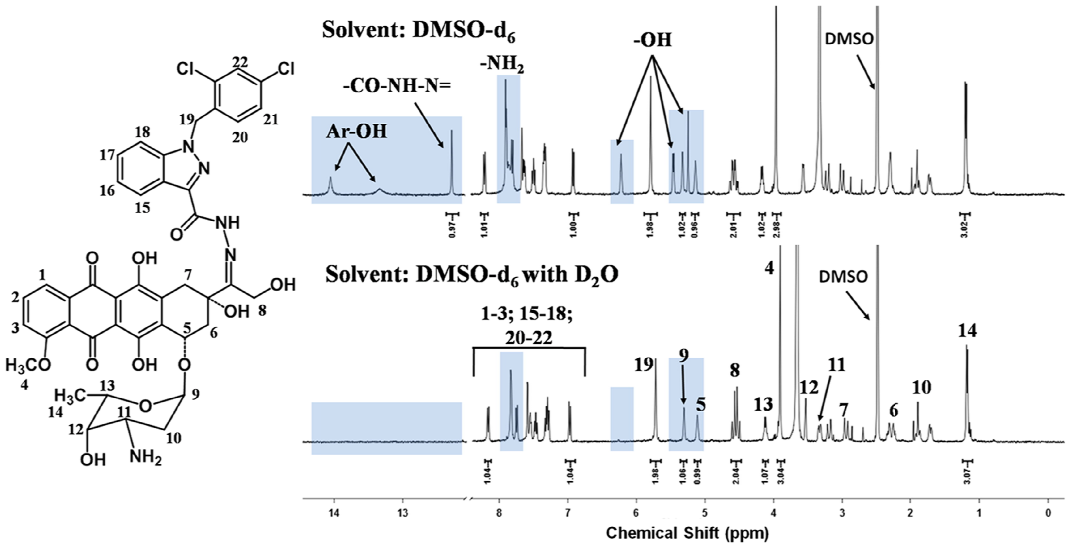

Fig.2 Comparison of the ^{1}H-NMR spectra of ADD-DOX dissolved in DMSO-d$_6$ with or without D$_2$O. Areas related to the signals of active protons were highlighted as blue.

This journal is © The Royal Society of Chemistry [year]

Journal of Materials Chemistry B Accepted Manuscript

Cite this: DOI: 10.1039/c0xx00000x

www.rsc.org/xxxxxx

ARTICLE TYPE

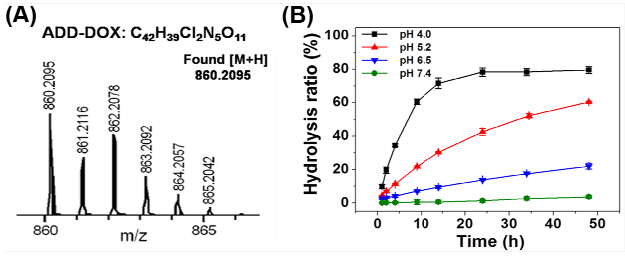

Fig.3 (A) HR-ESI-MS spectrum of ADD-DOX (positive mode) with m/z values ranging from 860 to 866. **(B)** Hydrolysis kinetics of ADD-DOX in water/methanol (75/25, v/v) at different pH values.

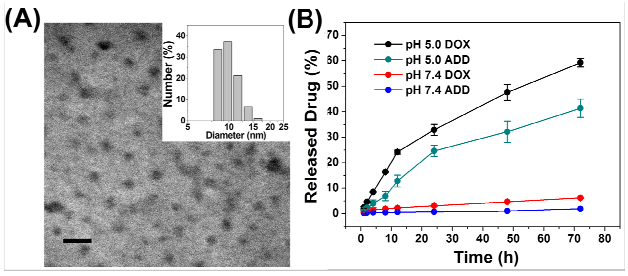

Fig.4 (A) Representative TEM micrograph of ADD-DOX (M) with staining treatment of phosphotungstic acid solution (1%, m/m), Scale bar represented 50 nm; inset indicated the hydrodynamic size distribution of ADD-DOX (M) in PBS solution. **(B)** Drug release kinetics of ADD-DOX (M) incubated in aqueous solution at pH 5.0 or 7.4. Released ADD and DOX were quantified by HPLC and fluorescent spectrophotometry, respectively.

To verify the generation of hydrazone bond between ADD and DOX, we determined the active protons in the structure of product through comparing the ^{1}H-NMR spectra obtained in DMSO-d_6 with or without D_2O (Fig. 2, related areas were highlighted as blue). For the proton in the amide group (-CO-NH-), a significant downfield shifting from δ=9.6 (seen in Fig. S2) to 12.2 ppm appeared after the reaction, which should be attributed to the deshielding effect resulting from the new generated 'C=N' bond. On the other hand, the amino protons in the hydrazide group of ADD possessed a resonance peak with integration of 2H at δ=4.4 (N-H_2 in Fig. S2) but no signal in the spectrum of the final product (Fig. 2), indicating the entirely depletion of hydrazide groups within the conjugation process. These results clearly verified the existence of hydrazone bond in the final product.

Next we examined the obtained product by high resolution mass spectroscopy to determine its mass and molecular formula. We have found a protonated species with exact mass (M+H) of 860.2095. This value matched well with the molecular weight that calculated according to the chemical formula of ADD-DOX ($C_{42}H_{39}Cl_2N_5O_{11}$, M+H: 860.2101). Fig. 3A showed the detailed signal distribution of such protonated species (m/z from 860 to 866), which were precisely consistent with that existed in the theoretical isotope pattern of ADD-DOX (Fig. S4A). In addition, we also observed signals within the interval from 690 to 740 (m/z), which should be attributed to the possible molecular fragments of ADD-DOX (Fig. S4B). These thus demonstrated that the obtained product possessed the same mass and molecular formula as of ADD-DOX.

Since hydrazone bond is well known as a cleavable bond with acid-catalyzed hydrolysis property, we next investigated the hydrolysis profile of our product. The experiments were performed in water/methanol (75/25, v/v) with different pH values and the results were evaluated by HPLC. Fig. 3B showed relative hydrolysis kinetics of our product under different pH values. The hydrolysis rate was found to be significantly faster under more acidic environment: nearly 60% was cleaved into free ADD and DOX at pH 4.0 within the first 10 h, whereas less than 3% was hydrolyzed meanwhile at pH 7.4. This phenomenon matched well with the aforementioned hydrolysis property of hydrazone bond, thus providing another evidence for the conjugation of ADD and DOX. Besides HPLC, ^{1}H-NMR and HR-ESI-MS, other characterization including ^{13}C-NMR, FTIR, UV and fluorescent spectroscopy were also performed to verify the final product. The results and the corresponding discussion can be found in Fig. S5-S8. Taken these data collectively, we ascertained that the obtained product was exactly ADD-DOX as expected.

Preparation and characterization of ADD-DOX (M)

Upon completion of the synthesis and characterization, ADD-DOX conjugates were subsequently loaded by DSPE-PEG_{2000} micelles (denoted as ADD-DOX (M)). Schematic representation for the preparation of ADD-DOX (M) was shown in Fig. 1, Step B. ADD-DOX and DSPE-PEG_{2000} were co-dissolved in anhydrous methanol, followed by evaporation of solvent to obtain a uniform thin film. Then the film was treated by PBS (pH 7.4), allowing the self-assembly of ADD-DOX and DSPE-PEG_{2000} to form ADD-DOX (M). The encapsulation efficiency for such preparation approach was over 99% and the drug loading efficiency of ADD-DOX (M) could be readily adjusted by altering the inputted mass ratio of ADD-DOX to DSPE-PEG_{2000}. We prepared a type of micelles with drug loading efficiency of 16.7% (m/m) for the following characterization and cellular experiments. The as-prepared PBS solution of ADD-DOX (M) micelles was stored at 4 ºC before use. It was found that over 95% ADD-DOX still retained in micelles after storing for 2 weeks, indicating a well protective effect of this micelle formulation to the embedded ADD-DOX (Fig. S9).

The morphological feature of ADD-DOX (M) was characterized by TEM. Samples were treated with 0.1% phosphotungstic acid (PTA) for positive staining before observation. [35] As shown in Fig. 4A, ADD-DOX (M) (black dots) possessed nearly spherical morphology and mono-dispersion characteristic. The average hydrodynamic size (corresponding size distribution shown as inset) and zeta potential of ADD-DOX (M) in aqueous solution were determined to be 11.2 ± 0.5 nm and

Journal of Materials Chemistry B Accepted Manuscript

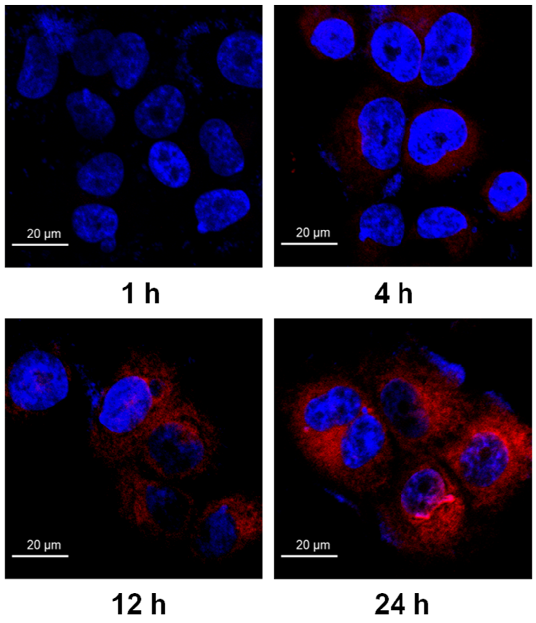

Fig. 5 Fluorescent images of MCF-7/ADR cells that incubated with ADD-DOX (M) (equivalent with ADD-DOX concentration of 5 μM) for time periods ranging from 1 to 24 h. Blue and red fluoresce represented the localization of nuclei and ADD-DOX (M), respectively.

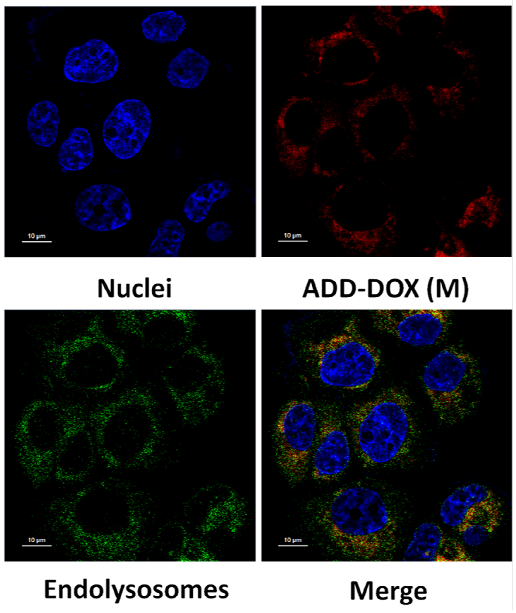

Fig.6 Intracellular localization of ADD-DOX (M) in MCF-7/ADR cells. Cells were incubated with culture medium containing ADD-DOX (M) (equivalent with 40 μM ADD-DOX) for 4h before observation by CLSM. The localization of nuclei, ADD-DOX (M) and endolysosomes were indicated by blue, red and green fluorescence, respectively.

-7.4 ± 1.2 mV, respectively, by DLS method.

The drug release behaviors of ADD-DOX (M) were examined through a dialysis method. The pH values of the outer phases were set as 5.0 and 7.4 to mimic that of endolysosomes and physiological environment, respectively. At pre-designed time points, samples were withdrawn from outer phases and the concentrations of ADD and DOX were analyzed by HPLC and fluorescent spectrophotometry, respectively. Since there was negligible ADD-DOX retained in separated samples (detected by HPLC, data not shown), the fluorescence should only be attributed to DOX. Fig. 4B illustrated the drug release kinetics of ADD-DOX (M). After 72 h of incubation at 37 °C, less than 6% of DOX and 2% of ADD were released at pH 7.4, indicating the low leakage of drugs from ADD-DOX (M) under physiological pH value. Compared to this, over 60% of DOX and 40% of ADD were released at pH 5.0, which suggested that ADD-DOX (M) would rapidly release free individual drugs in moderate acidic environment. This acid-responsive drug release characteristic of ADD-DOX (M) was probably related to the charge of ADD-DOX and DSPE-PEG_{2000}. When pH reduced from 7.4 to 5.0, more amino groups (in the sugar ring of DOX moiety) were protonated, which strengthened the electronic repulsion among ADD-DOX molecules and thus enhanced the dissociation of such embedded drug conjugates; on the other hand, the charge of DSPE-PEG_{2000} (isoelectric points of ~5.9) changed from negative to weak positive, which eliminated their electrostatic attraction to ADD-DOX. [33] As a result, the embedded ADD-DOX conjugates in micelles would expose to aqueous solution, thus promoting its hydrolysis and the following release of free ADD and DOX. In addition, because DOX possesses higher water solubility, it is expected that DOX will more readily diffuse into solution from the polymer matrix and thereby holds a faster release rate than that of ADD at the same pH condition. This is confirmed by the experimental result shown in Fig. 4B.

Cellular endocytosis of ADD-DOX (M)

Next, we examined the internalization of ADD-DOX (M) by drug-resistant cancer cells. MCF-7/ADR cell line, a representative DOX-related drug-resistant cancer model, was used for this study. Cells were cultured with ADD-DOX (M) for diverse time periods and imaged by CLSM. As shown in Fig. 5, nuclei and ADD-DOX (M) were indicated as blue and red fluorescence, respectively. With prolonging incubation time, the intracellular red fluorescence enhanced substantially. The corresponding mean fluorescence intensities (MFI) in cells were determined by FCM and the results were shown in Fig. S10. The time-dependent increase of MFI values agreed with the results of CLSM observation, indicating the gradual accumulation of ADD-DOX (M) micelles in MCF-7/ADR cells.

To confirm that the internalization of ADD-DOX (M) was realized by cellular endocytosis, we treated MCF-7/ADR cells with such micelles at different temperatures (4 ºC and 37 ºC). After incubation for 1 h, the fluorescence in cells was determined by both CLSM (Fig. S11A) and FCM (Fig. S11B). In sharp contrast, distinct red fluorescence was detected in cells treated at 37 ºC, whereas only weak fluorescence signals existed in cells treated at 4 ºC. This significant decrease for the entry of ADD-DOX (M) into cells at lower temperature suggested that such micelles were internalized by cells via a temperature-dependent endocytic pathway. [16, 33]

After endocytosis by tumor cells, nanocarriers generally exist in endosomes. These intracellular compartments can fuse with a type of acidic organelles known as lysosomes to form endolysosomes. [36] Since acidic environment in endolysosomes was crucial for the rapid release of free individual drugs as proven above (Fig. 4B), we investigated the subcellular localization of ADD-DOX (M). MCF-7/ADR cells were incubated with ADD-DOX (M) for 4 h. Thereafter, those cells

This journal is © The Royal Society of Chemistry [year]

Journal of Materials Chemistry B Accepted Manuscript

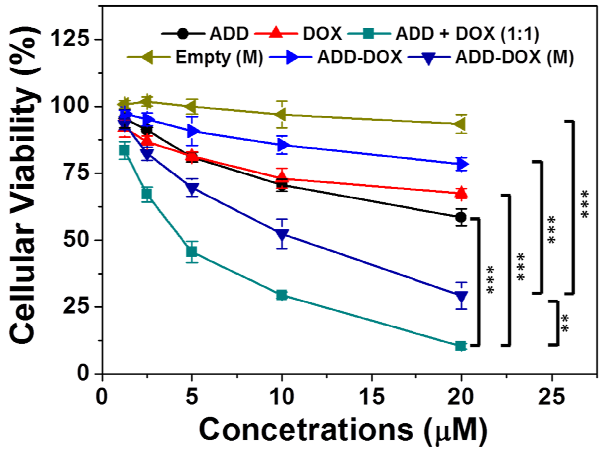

Fig. 7 Cellular viabilities of MCF-7/ADR cells that incubated for 72 h with different doses (ranging from 1.25 to 20 μM) of ADD, DOX, the mixture of ADD and DOX (molar ratio of 1:1), ADD-DOX conjugates, empty DSPE-PEG_{2000} micelles (denoted as empty (M)) and ADD-DOX (M). For the group of empty (M), the concentrations of DSPE-PEG_{2000} ranged from 6.3 to 100 μg/mL (equivalent with drug concentration of 1.25 to 20 μM). ** <0.01; *** p<0.001, n=6.

were exposed to Lysotracker Green and Hoechst 33258 in sequence for staining endolysosomes/lysosomes and nuclei, respectively, followed by CLSM observation. The localization of nuclei, ADD-DOX (M) and endolysosomes were shown in Fig. 6 and indicated as blue, red and green fluorescence, respectively. In the merged image, there were numerous yellow dots (overlying of red and green), indicating that abundant ADD-DOX (M) existed within endolysosomes after cellular endocytosis.

Overcoming MDR by ADD-DOX (M)

In following studies, we evaluated the cytotoxicity of ADD-DOX (M) to MCF-7/ADR cells. Cells were exposed to drugs with concentrations ranging from 1.25 to 20 μM for 72 h before the determination of cellular viabilities by MTT assay. DMSO was added into culture medium to facilitate the dissolution of ADD (0.1%, v/v) or ADD-DOX conjugates (0.5%, v/v). For better comparison, the group of free DOX was also cultured in medium containing 0.1% DMSO (existence of DMSO exhibited no significant influence to the cytotoxicity of DOX, seen in Fig. S12). As shown in Fig. 7, the cytotoxicity of the drugs mixture of ADD and DOX (molar ratio 1:1) was remarkably higher than that of individual ADD or DOX at the same drug concentrations. The IC_{50} value of the drug mixture was 4.3 μM, which were 9.1 and 17.1 folds lower than that of free ADD (39.1 μM) and DOX (73.7 μM), respectively. This thus verified the combinational anti-MDR effect of ADD and DOX.

Since it is documented that the hydrazide group is a bio-functional moiety of ADD, [30] ADD-DOX conjugates must convert to free ADD to impede mitochondrial function and mediate combination therapy. Therefore, the cytotoxicity of ADD-DOX relies on its hydrolysis behaviors. As mentioned above, ADD-DOX conjugates held acid-responsive hydrolysis characteristic (Fig. 3B). It was hypothesized that applying ADD-DOX (M) to cells might lead to much higher inhibitory effect than application of free ADD-DOX conjugates, because ADD-DOX (M) would exist within endolysosomes but free ADD-DOX might directly diffuse into cytoplasm. [21] This matched well with the results shown in Fig. 7. The IC_{50} value of ADD-DOX (M) was 10.1 μM, which was about 12.1 folds lower than that of free ADD-DOX conjugates (IC_{50}, 121.4 μM). Of particular note that the empty DSPE-PEG_{2000} micelles (denoted as empty (M)) showed negligible toxicity to cells, the cytotoxicity of ADD-DOX (M) was only attributed to the loaded ADD-DOX conjugates. Moreover, we also observed that the cytotoxicity of ADD-DOX (M) was a bit lower than that of the drug mixture, which probably resulted from that a portion of drugs was still embedded in micelles after incubation for 72 h (drug release following the pH=5.0 profile in Fig. 4B). To specifically evaluate the anti-MDR capability of ADD-DOX (M), we then calculated the resistance factor (denoted as RF) of ADD-DOX (M). Low RF value generally represents high activity in overcoming MDR. [16, 37] According to the data shown in Fig. S13, the RF value of DOX was 80.1, verifying the serious resistance of MCF-7/ADR cells to this chemo-drug. In marked contrast, the RF value of ADD-DOX (M) was 2.7, about 29.9-folds lower than that of free DOX, indicating that ADD-DOX (M) possessed robust anti-MDR capability.

To further confirm that the excellent anti-MDR capability of ADD-DOX (M) related to the release of ADD and DOX, we examined whether ADD-DOX (M) possessed the same therapeutic functions as of ADD and DOX. Since inhibition of ATP production is among the most direct evidences for ADD to impede mitochondria, we evaluated the intracellular ATP level of cells treated by ADD-DOX (M). As shown in Fig. S14, distinct decreases of the intracellular ATP level were observed in the groups of ADD (29.2%), drugs mixture (31.1%) and ADD-DOX (M) (24.4%), whereas no significant change was found in the group of DOX. These suggested that the down-regulation of ATP level in MCF-7/ADR cells was only attributed to ADD. Additionally, we found that the ATP level underwent a sharp decrease (67.1%) in cells treated with higher dose of ADD-DOX (M), which further confirmed the mitochondria-inhibitory function of ADD-DOX (M). On the other hand, since the widely known pharmacological mechanism of DOX is the entry of this drug into nuclei to inhibit DNA replication, we performed CLSM observation on MCF-7/ADR cells treated by ADD-DOX (M) for 48 h. As shown in Fig. S15A, Red fluorescence appeared in both the nuclei and the cytoplasm, which is similar to that distributing in cells treated by free DOX under the same conditions (Fig. S15B). Comparatively, in cells that incubated with ADD-DOX (M) for shorter time periods (such as 1h and 4 h), red fluorescence only existed in the cytoplasm as shown in Fig. S11A and Fig. 6, respectively. These clearly verified that ADD-DOX (M) could also act on nucleic acids.

Taken together all the above *in vitro* experiments, we utilized a schematic illustration to describe the intracellular behaviors of ADD-DOX (M) in drug-resistant cells (Fig. 1, Step C): (1) ADD-DOX (M) were internalized by cells via endocytic pathway; (2) endosomes fused with lysosomes to form endolysosomes; (3) ADD-DOX hydrolyzed into ADD and DOX within endolysosomes, accompanied with the release of such two individual drugs into cytoplasm; (4) released ADD and DOX acted on mitochondria and nucleic acids, respectively. With these intracellular processes, ADD-DOX (M) exhibited remarkable inhibitory effect to MDR cancer cells. Besides the robust *in vitro*

Journal of Materials Chemistry B Accepted Manuscript

anti-MDR capability, ADD-DOX (M) formulation also possessed other characteristics, including good biocompatibility and safety (as the component DSPE-PEG_{2000} has been certified for human use), excellent stability and low leakage in physiological condition, etc. These thus enabled the potential application of ADD-DOX (M) for *in vivo* anti-MDR study. However, to better achieve this purpose, it is still necessary to diminish unexpected side effects (such as unspecific accumulation in healthy tissues) via improving the delivery system. Relative works are being carried out in our laboratory.

Conclusions

In conclusions, we demonstrated the synthesis and characterization of ADD-DOX conjugates, which possessed acid-responsive hydrolysis property. These drug conjugates can be readily encapsulated by conventional DSPE-PEG_{2000} nanocarriers with high drug encapsulation efficiency and well controllable drug loading efficiency. The obtained ADD-DOX (M) micelles were stable at physiological pH value, but can rapidly release free ADD and DOX under mild acidic environment. After endocytosis by cells, ADD-DOX (M) exhibited more efficient anti-MDR capability as compared to free ADD-DOX conjugates, which should be attributed to the accelerated hydrolysis rate of drug conjugates in endolysosomes. To sum up, we for the first time reported the combinational use of Adjudin and Doxorubicin for MDR cancer treatment and we also developed a novel formulation via incorporating drug conjugation approach and nanocarrier technology to efficiently co-deliver such two drugs.

Acknowledgements

This work was supported by National Basic Research Program of China (973 Program, 2012CB932501, 2013CB945604), NSFC (21204024, 81373360, 81301306 and 31270032), Doctoral Fund of Ministry of Education of China 45 (20120142120093), Innovative Research Fund, Chutian Scholar Award, 2013 Youth Scholar Award of HUST, SJTU Interdisciplinary Research Grant (YG2012ZD05), and Postdoctoral Science Foundation of China (2013M531693).

Notes and references

a Tongji School of Pharmacy; National Engineering Research Center for Nanomedicine, Huazhong University of Science and Technology, Wuhan 430030, P.R. China. Fax & telephone: +86-027-83601832. E-mail: zhipingzhang@mail.hust.edu.cn.

b The Mary M. Wohlford Laboratory for Male Contraceptive Research, Center for Biomedical Research, Population Council, New York, NY 10065, USA.

c State Key Laboratory of Oncogenes and Related Genes, Renji-Med X Clinical Stem Cell Research Center, Ren Ji Hospital, School of Medicine; School of Biomedical Engineering & Med-X Research Institute, Shanghai Jiao Tong University, Shanghai 200030, P.R. China.

Electronic Supplementary Information (ESI) available: [experimental details, characterization and cytotoxicity of prodrug, fluorescent microscopy images and flow cytometry data]. DOI: 10.1039/b000000x/

1. C. Holohan, S. Van Schaeybroeck, D. B. Longley and P. G. Johnston, *Nat. Rev. Cancer*, 2013, **13**, 714-726.
2. X.-B. Xiong and A. Lavasanifar, *ACS Nano*, 2011, **5**, 5202-5213.
3. A. M. Chen, M. Zhang, D. Wei, D. Stueber, O. Taratula, T. Minko and H. He, *Small*, 2009, **5**, 2673-2677.
4. H. Zhu, H. Chen, X. Zeng, Z. Wang, X. Zhang, Y. Wu, Y. Gao, J. Zhang, K. Liu and R. Liu, *Biomaterials*, 2014, **35**, 2391-2400.
5. G. Navarro, R. R. Sawant, S. Biswas, S. Essex, C. Tros de Ilarduya and V. P. Torchilin, *Nanomedicine*, 2012, **7**, 65-78.
6. C.-M. J. Hu and L. Zhang, *Biochem. Pharmacol.*, 2012, **83**, 1104-1111.
7. Z. J. Deng, S. W. Morton, E. Ben-Akiva, E. C. Dreaden, K. E. Shopsowitz and P. T. Hammond, *ACS nano*, 2013, **7**, 9571-9584.
8. N. R. Patel, A. Rathi, D. Mongayt and V. P. Torchilin, *Int. J. Pharm.*, 2011, **416**, 296-299.
9. D. C. Wallace, *Nat. Rev. Cancer*, 2012, **12**, 685-698.
10. R.-h. Xu, H. Pelicano, Y. Zhou, J. S. Carew, L. Feng, K. N. Bhalla, M. J. Keating and P. Huang, *Cancer Res.*, 2005, **65**, 613-621.
11. D. D. Mruk, C.-H. Wong, B. Silvestrini and C. Y. Cheng, *Nat. Med.*, 2006, **12**, 1323-1328.
12. K.-W. Mok, D. D. Mruk, P. P. Lie, W.-Y. Lui and C. Y. Cheng, *Reproduction*, 2011, **141**, 571-580.
13. Q. R. Xie, Y. Liu, J. Shao, J. Yang, T. Liu, T. Zhang, B. Wang, D. D. Mruk, B. Silvestrini and C. Y. Cheng, *Biochem. Pharmacol.*, 2013, **85**, 345-355.
14. G. Minotti, P. Menna, E. Salvatorelli, G. Cairo and L. Gianni, *Pharmacol. Rev.*, 2004, **56**, 185-229.
15. X. Duan, J. Xiao, Q. Yin, Z. Zhang, H. Yu, S. Mao and Y. Li, *ACS Nano*, 2013, **7**, 5858-5869.
16. F. Peng, Y. Su, X. Ji, Y. Zhong, X. Wei and Y. He, *Biomaterials*, 2014, **35**, 5188-5195.
17. D. Peer, J. M. Karp, S. Hong, O. C. FaroKhzad, R. Margalit and R. Langer, *Nature Nanotechnol.*, 2007, **2**, 751-760.
18. V. P. Torchilin, *Nat. Rev. Drug Discov.*, 2014, **13**, 813-827.
19. M. L. Hans and A. M. Lowman, *Curr. Opin. Solid St. M.*, 2002, **6**, 319-327.
20. M. B. Zheng, C. X. Yue, Y. F. Ma, P. Gong, P. F. Zhao, C. F. Zheng, Z. H. Sheng, P. F. Zhang, Z. H. Wang and L. T. Cai, *Acs Nano*, 2013, **7**, 2056-2067.
21. S. Aryal, C.-M. J. Hu, V. Fu and L. Zhang, *J. Mater. Chem.*, 2012, **22**, 994-999.
22. J. Park, S. H. Wrzesinski, E. Stern, M. Look, J. Criscione, R. Ragheb, S. M. Jay, S. L. Demento, A. Agawu, P. L. Limon, A. F. Ferrandino, D. Gonzalez, A. Habermann, R. A. Flavell and T. M. Fahmy, *Nature Mater.*, 2012, **11**, 895-905.
23. V. P. Torchilin, *Nat. Rev. Drug Discov.*, 2005, **4**, 145-160.
24. Y. Mi, J. Zhao and S.-S. Feng, *Nanomedicine*, 2013, **8**, 1559-1562.
25. R. Mo, T. Jiang and Z. Gu, *Nanomedicine*, 2014, **9**, 1117-1120.
26. Q. Cheng, H. Shi, H. Wang, Y. Min, J. Wang and Y. Liu, *Chem. Commun.*, 2014.
27. S. Dhar and S. J. Lippard, *P. Natl. Acad. Sci. USA*, 2009, **106**, 22199-22204.
28. K. Suntharalingam, Y. Song and S. J. Lippard, *Chem. Commun.*, 2014, **50**, 2465-2468.
29. S. Aryal, C. M. J. Hu and L. Zhang, *Small*, 2010, **6**, 1442-1448.
30. C. Y. Cheng, B. Silvestrini, J. Grima, M.-y. Mo, L.-j. Zhu, E. Johansson, L. Saso, M.-G. Leone, M. Palmery and D. Mruk, *Biol. Reprod.*, 2001, **65**, 449-461.
31. Q. Chen, D. A. Sowa, J. Cai and R. Gabathuler, *Synth. Commun.*, 2003, **33**, 2377-2390.
32. D. Willner, P. A. Trail, S. J. Hofstead, H. D. King, S. J. Lasch, G. R. Braslawsky, R. S. Greenfield, T. Kaneko and R. A. Firestone, *Bioconjugate Chem.*, 1993, **4**, 521-527.
33. T. Wei, J. Liu, H. Ma, Q. Cheng, Y. Huang, J. Zhao, S. Huo, X. Xue, Z. Liang and X.-J. Liang, *Nano Lett.*, 2013, **13**, 2528-2534.
34. N. Tang, G. Du, N. Wang, C. Liu, H. Hang and W. Liang, *J. Natl. Cancer Inst.*, 2007, **99**, 1004-1015.
35. X. Li, Y. Chen, M. Wang, Y. Ma, W. Xia and H. Gu, *Biomaterials*, 2013, **34**, 1391-1401.
36. I. Mellman, *Annu. Rev. Cell Dev. Biol.*, 1996, **12**, 575-625.
37. F. M. Kievit, F. Y. Wang, C. Fang, H. Mok, K. Wang, J. R. Silber, R. G. Ellenbogen and M. Zhang, *J. Control. Release*, 2011, **152**, 76-83.

Journal of Materials Chemistry B Accepted Manuscript

This journal is © The Royal Society of Chemistry [year]

Table of contents entry

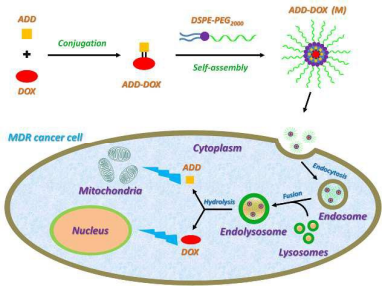

We integrate drug conjugation and nanocarrier approaches to co-deliver Adjudin and Doxorubicin for the treatment of drug-resistant cancer cells.

Journal of Materials Chemistry B Accepted Manuscript